Anti-Hebbian Long-Term Potentiation in the Hippocampal Feedback Inhibitory Circuit

Karri P. Lamsa[1], **Joost H. Heeroma**[1], **Peter Somogyi**[2], **Dmitri A. Rusakov**[1], and **Dimitri M. Kullmann**[1],*

[1]Institute of Neurology, University College London, Queen Square, London WC1N 3BG, UK

[2]Anatomical Neuropharmacology Unit, Medical Research Council, Oxford University, Mansfield Road, Oxford OXI 3HT, UK

Abstract

Long-term potentiation (LTP), which approximates Hebb's postulate of associative learning, typically requires depolarization-dependent glutamate receptors of the NMDA (*N*-methyl-D-aspartate) subtype. However, in some neurons, LTP depends instead on calcium-permeable AMPA-type receptors. This is paradoxical because intracellular polyamines block such receptors during depolarization. We report that LTP at synapses on hippocampal interneurons mediating feedback inhibition is "anti-Hebbian": It is induced by presynaptic activity but prevented by postsynaptic depolarization. Anti-Hebbian LTP may occur in interneurons that are silent during periods of intense pyramidal cell firing, such as sharp waves, and lead to their altered activation during theta activity.

Associative *N*-methyl-D-aspartate receptor (NMDAR)–dependent LTP is induced by coincident activity in afferent pathways sufficient to depolarize postsynaptic neurons (1). However, the voltage dependence of Ca^{2+}-permeable α-amino-3-hydroxy-5-methyl-4-isoxazolepropionic acid receptors (CP-AMPARs) is opposite to that of NMDARs (2, 3). Because CP-AMPARs are blocked by cytoplasmic polyamines upon depolarization (4, 5), maximal Ca^{2+} influx occurs when the membrane potential is relatively negative. LTP dependent on CP-AMPARs occurs in interneurons of the spinal cord and amygdala (6, 7), but its postsynaptic voltage dependence has not been explored. In hippocampal interneurons, CP-AMPARs have been implicated in long-term depression (8-10), and contribute to synaptic Ca^{2+} transients, especially in the stratum oriens/alveus (11). Many interneurons in the oriens/alveus also show NMDAR-independent LTP (12). We therefore looked for associative LTP in these cells, while recording with the gramicidin perforated patch technique to preserve intracellular polyamines (13).

Stimulation of pyramidal cell axon collaterals in the alveus evoked monosynaptic excitatory postsynaptic potentials (EPSPs) subthreshold for evoking action potentials. After recording a baseline, we paired high-frequency burst (HFB) stimulation (five pulses at 100 Hz, repeated 20 times) with stimulation of a second, supra-threshold, alveus pathway. "In-phase" associative pairing (phase difference $\Delta\Phi = 0°$) failed to elicit associative LTP in either pathway ($n = 7$; Fig. 1, A and B). In a further set of experiments, we alternately stimulated

two weak pathways, and then delivered HFBs to both pathways antiphase ($\Delta\Phi = 180°$). This evoked a persistent increase in EPSP initial slope in one or both pathways in all cells ($n = 7$; Fig. 1, C and D). LTP was elicited even when HFB stimuli were delivered to only one weak pathway ($n = 7$; Fig. 1, E and F). Thus, LTP at excitatory synapses on interneurons in the oriens/alveus is prevented by associative pairing, in direct contrast to NMDAR-dependent LTP (1).

Can direct manipulation of the postsynaptic membrane potential similarly gate LTP induction? We delivered HFBs to one pathway coinciding with the trough (somatic voltage: −90 mV) of an imposed 4-Hz sinusoidal somatic membrane potential oscillation. HFBs were then delivered to the other pathway coinciding with the depolarizing phase. In 8 out of 11 cells, pairing with hyperpolarization, but not with depolarization, resulted in LTP (Fig. 2, A and B). One cell showed the opposite behavior, and the other two showed no effect of either pairing (fig. S1). Single alveus stimuli in phase with maximum hyperpolarization (100 times) also induced LTP ($n = 10$; Fig. 2C), but pairing with depolarization was ineffective (Fig. 2D). Thus, even low-frequency stimulation can trigger LTP if interneurons are hyperpolarized.

Because the induction requirements for LTP in most interneurons in the oriens/alveus are diametrically opposite to Hebb's postulate (14, 15), we refer to it as "anti-Hebbian." We tested the same LTP induction protocols in interneurons in the stratum radiatum. Hebbian LTP could be elicited in about half of these cells, many of which mediate feedforward inhibition (16), whereas pairing either HFB or low-frequency stimuli with hyperpolarization was uniformly unsuccessful (figs. S1 and S2). Anti-Hebbian LTP is thus characteristic of excitatory synapses made by local pyramidal cells on interneurons in the oriens/alveus but not of Schaffer collateral synapses on interneurons in the stratum radiatum.

Can differences in synaptic glutamate receptors explain whether Hebbian, anti-Hebbian, or no LTP is elicited? When interneurons in the oriens/alveus were recorded in whole-cell voltage clamp [with γ-aminobutyric acid (GABA) receptors blocked, and with spermine included in the pipette solution], synaptic AMPARs activated by alveus stimulation were generally strongly rectifying (Fig. 2E), consistent with expression of CP-AMPARs (11). Furthermore, only small NMDAR-mediated synaptic currents were detected at a positive holding potential, consistent with low synaptic expression of the NR1 subunit (17).

We tested interneurons in the oriens/alveus, recorded in perforated patch mode, with a further anti-Hebbian protocol High-frequency stimulation of one alveus pathway (100 Hz, 100 pulses, delivered twice) paired with hyperpolarization, with NMDARs blocked, elicited LTP in 25 out of 31 cells (Figs. 3A and 4C). We repatched 11 of these cells in whole-cell voltage-clamp mode and found pronounced synaptic AMPAR rectification in every cell where anti-Hebbian LTP was evoked. The rectification index did not differ detectably between control and potentiated pathways (Fig. 3B), yielding no evidence for an LTP-related change in the permeability of synaptic AMPARs to Ca^{2+} (18).

In contrast, repatched interneurons in the stratum radiatum generally showed nonrectifying AMPARs and a large NMDAR-mediated component of Schaffer collateral-evoked synaptic currents (fig. S2) (9). The anti-Hebbian LTP induction protocol was successful in only 2 out of 20 cells in the stratum radiatum. AMPARs at Schaffer collateral synapses on 11 cells (none of which showed anti-Hebbian LTP) were nonrectifying (fig. S3).

Anti-Hebbian LTP thus typically occurs at synapses on interneurons in the oriens/alveus equipped with rectifying CP-AMPARs. Are these a uniform subgroup? Seven interneurons were regular-spiking oriens-lacunosum molecular (O-LM) cells (Fig. 3C, fig. S4), which mediate feedback inhibition of the apical dendrites of pyramidal neurons (19). Twelve other

interneurons had horizontal dendrites and electrophysiological properties typical of O-LM cells, but axon visualization was incomplete (fig. S5). Anti-Hebbian LTP, however, also occurred in 17 out of 24 fast-spiking interneurons in the strata oriens or pyramidale, including one anatomically confirmed axo-axonic and two basket cells, which are innervated by CA1 pyramidal cells and target their perisomatic area. Seven other cells could not be classified.

Anti-Hebbian LTP is, however, rare at Schaffer collateral synapses on interneurons in the stratum radiatum, which generally mediate feedforward inhibition and express nonrectifying receptors (Fig. 3, D and E). Synaptic responses evoked by stratum radiatum stimulation in fast-spiking interneurons in the stratum pyramidale, however, had strongly rectifying AMPARs and a small NMDA component, and the Hebbian LTP induction protocol was uniformly unsuccessful ($n = 4$; fig. S6).

Does rectification of CP-AMPARs fully explain the anti-Hebbian nature of LTP in interneurons in the oriens/alveus? We first verified that AMPA/kainate receptors are necessary for induction, by pairing HFS with postsynaptic hyperpolarization while AMPA/kainate receptors were blocked with 2,3-dihydroxy-6-nitro-7-sulfamoylbenzo[f]quinoxaline (NBQX, 5 µM): After washout of the antagonist, EPSPs in the tetanized and control pathways recovered to the same extent ($n = 7$; Fig. 3F). We then explored systematically the voltage dependence of LTP. In five cells in the oriens/alveus where anti-Hebbian LTP was evoked in one alveus pathway, subsequent pairing of the other pathway with depolarization only evoked short-lived post-tetanic potentiation (Fig. 4A). In six other cells, pairing the second pathway with hyperpolarization elicited robust LTP in all cases (Fig. 4, B and C). We then adapted this experimental design to explore the effect of manipulating the rectification properties of CP-AMPARs. Having demonstrated anti-Hebbian LTP in one pathway, we repatched the interneuron in whole-cell mode either with or without spermine in the pipette solution. Following a short baseline recording (7 min from patch rupture), we then paired HFS of the second pathway either with depolarization (+20 mV) or with hyperpolarization (−90 mV). When spermine was omitted, pairing with depolarization evoked LTP in five out of five cells (Fig. 4D), consistent with Ca^{2+} influx via CP-AMPARs rendered non-rectifying by removal of polyamines (4). In contrast, HFS paired with depolarization failed to elicit LTP in five cells that were repatched with a spermine-containing pipette (Fig. 4E). In five other interneurons repatched with a spermine-containing solution, pairing HFS of the second pathway with hyperpolarization to −90 mV evoked LTP (Fig. 4F).

Polyamine-mediated rectification of AMPARs (and/or kainate receptors) thus explains the voltage dependence of LTP induction in these interneurons and reconciles our results with previous reports that a Hebbian protocol induces LTP in interneurons in the oriens/alveus when recorded with a polyamine-free whole-cell pipette solution (12). Also consistent with these reports, blockade of group I metabotropic glutamate receptors prevented LTP induction in interneurons with horizontal dendrites in the oriens/alveus (fig. S7). Finally, we looked for evidence that anti-Hebbian LTP is accompanied by an increase in glutamate-release probability (12), by applying extracellular polyamines, which also block CP-AMPARs in a use-dependent manner (20). After inducing anti-Hebbian LTP in one pathway, bath perfusion of N-(4-hydroxyphenylpropanoyl)-spermine (5 to 10 µM) caused a progressive decrease in EPSP initial slope, which was significantly faster in the paired than in the control pathway ($n = 7$; fig. S8). Given that anti-Hebbian LTP did not alter AMPAR rectification (Fig. 3B), this result is consistent with presynaptic expression.

Anti-Hebbian LTP may play distinct roles in neurons that show characteristic phase relationships in different network states (21, 22). During sharp-wave ripples, O-LM cells are

typically silent, while many of their input pyramidal neurons fire at high frequency (21), possibly satisfying the induction conditions for anti-Hebbian LTP. Binding of pyramidal neurons to a spatial map may occur during periods of high-frequency firing (23), similar to sharp-wave ripples. In contrast, during theta activity, which is associated with exploratory behavior (24), O-LM cells fire in phase with pyramidal cells (21) and may contribute to this oscillation through phase-locked dendritic inhibition (25). Anti-Hebbian LTP induced during ripples may therefore result in a long-term alteration of pyramidal cell excitation of O-LM cells, which persists during theta activity, and may therefore contribute to spatial memory formation, the early stages of which have been shown to withstand NMDAR blockade (26).

Supplementary Material

Refer to Web version on PubMed Central for supplementary material.

Acknowledgments

References

1. Bliss TV, Collingridge GL. Nature. 1993; 361:31. [PubMed: 8421494]

2. Jonas P, Racca C, Sakmann B, Seeburg PH, Monyer H. Neuron. 1994; 12:1281. [PubMed: 8011338]

3. Washburn MS, Numberger M, Zhang S, Dingledine R. J. Neurosci. 1997; 17:9393. [PubMed: 9390995]

4. Donevan SD, Rogawski MA. Proc. Natl. Acad. Sci. U.S.A. 1995; 92:9298. [PubMed: 7568121]

5. Bowie D, Mayer ML. Neuron. 1995; 15:453. [PubMed: 7646897]

6. Gu JG, Albuquerque C, Lee CJ, MacDermott AB. Nature. 1996; 381:793. [PubMed: 8657283]

7. Mahanty NK, Sah P. Nature. 1998; 394:683. [PubMed: 9716132]

8. Laezza F, Doherty JJ, Dingledine R. Science. 1999; 285:1411. [PubMed: 10464102]

9. Lei S, McBain CJ. Neuron. 2002; 33:921. [PubMed: 11906698]

10. Laezza F, Dingledine R. J. Neurophysiol. 2004; 92:3575. [PubMed: 15331617]

11. Topolnik L, Congar P, Lacaille JC. J. Neurosci. 2005; 25:990. [PubMed: 15673681]

12. Perez Y, Morin F, Lacaille JC. Proc. Natl. Acad. Sci. U.S.A. 2001; 98:9401. [PubMed: 11447296]

13. Materials and methods are available as supporting material on Science Online.

14. Hebb, DO. The Organization of Behavior. Wiley; New York: 1949.

15. Bi G, Poo M. Annu. Rev. Neurosci. 2001; 24:139. [PubMed: 11283308]

16. Lamsa K, Heeroma JH, Kullmann DM. Nat. Neurosci. 2005; 8:916. [PubMed: 15937481]

17. Nyiri G, Stephenson FA, Freund TF, Somogyi P. Neuroscience. 2003; 119:347. [PubMed: 12770551]

18. Plant K, et al. Nat. Neurosci. 2006; 9:602. [PubMed: 16582904]

19. Blasco-Ibanez JM, Freund TF. Eur. J. Neurosci. 1995; 7:2170. [PubMed: 8542073]

20. Mainen ZF, Jia Z, Roder J, Malinow R. Nat. Neurosci. 1998; 1:579. [PubMed: 10196565]

21. Klausberger T, et al. Nature. 2003; 421:844. [PubMed: 12594513]

22. Klausberger T, et al. Nat. Neurosci. 2004; 7:41. [PubMed: 14634650]

23. Dragoi G, Harris KD, Buzsaki G. Neuron. 2003; 39:843. [PubMed: 12948450]

24. Buzsaki G. Neuron. 2002; 33:325. [PubMed: 11832222]

25. Gillies MJ, et al. J. Physiol. 2002; 543:779. [PubMed: 12231638]

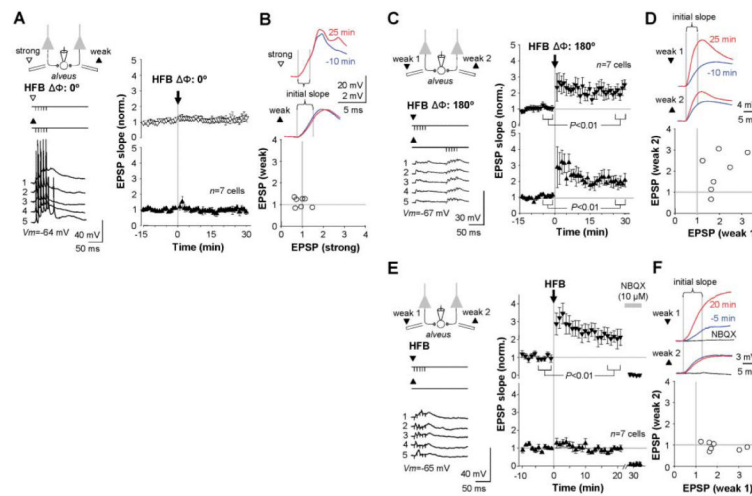26. Kentros C, et al. Science. 1998; 280:2121. [PubMed: 9641919]

Fig. 1.
Associative pairing precludes LTP in interneurons in the stratum oriens/alveus. (**A**) Left: Schematic illustrating in-phase high-frequency burst (HFB) stimulation of weak and strong alveus pathways (filled and open symbols, respectively). Sample traces (1 to 5) show action potentials evoked by pairing in one cell. Right: Baseline-normalized EPSP initial slopes (mean ± SEM). (**B**) Top: Averaged EPSPs recorded before (blue) and after (red) pairing in one cell, showing the interval used to measure the initial slope. Bottom: Baseline-normalized EPSP initial slopes (25 min after pairing) in the two pathways, plotted against one another. (**C**) Antiphase pairing of two weak pathways induced LTP in seven out of seven cells. Sample traces (left) are from one cell. (**D**) EPSPs before and after pairing and summary of results, plotted as in (B). (**E**) Burst stimulation of one pathway also induced LTP. AMPA/kainate receptors were blocked at the end of the experiment (NBQX), to verify that EPSP initial slopes were not contaminated by monosynaptic inhibition. (**F**) Effect of HFB stimulation of one pathway (weak 1), plotted as for (B) and (D). Traces (top) also show the effect of NBQX. Data in (C) (right) and (E) (right) are shown as the mean ± SEM. *V*m, membrane potential.
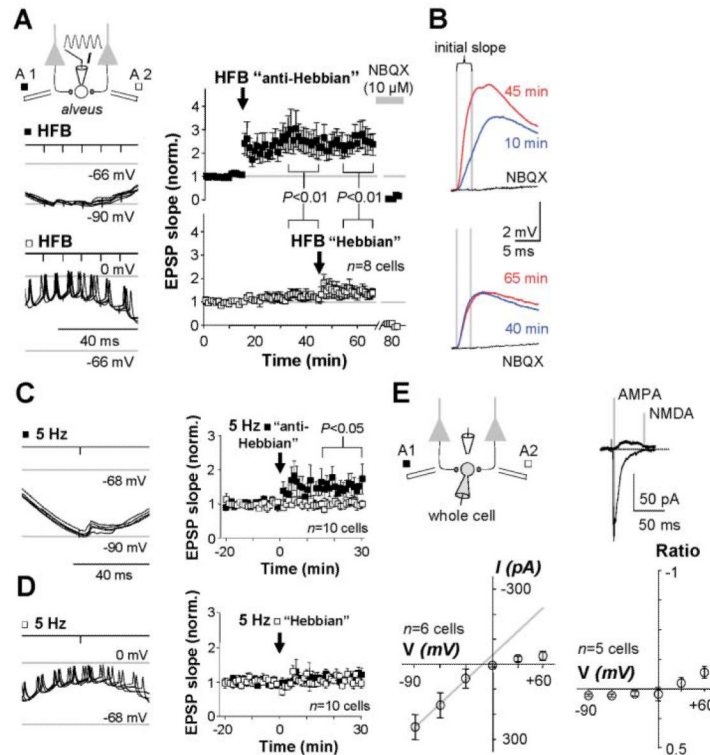
Fig. 2.

Postsynaptic membrane potential gates anti-Hebbian LTP induction. (**A**) LTP was evoked by pairing presynaptic stimulation with the hyperpolarizing but not the depolarizing phase of an imposed sinusoidal membrane potential oscillation. Left: Schematic and sample membrane potential traces during pairing in one cell (five sweeps superimposed for each pairing protocol). Right: Baseline-normalized EPSP initial slopes in eight cells showing LTP after anti-Hebbian pairing of HFB stimulation of one pathway with hyperpolarization. Subsequent Hebbian pairing of the other pathway with depolarization was ineffective. AMPA/kainate receptors were blocked at the end of the experiment (NBQX). Data are shown as the mean ± SEM. (**B**) Averaged EPSPs in one cell taken at the times indicated and after NBQX addition. Top: Anti-Hebbian pairing. Bottom: Hebbian pairing. (**C**) LTP was induced by pairing single stimuli at 5 Hz with hyperpolarization. Left: Sample traces during pairing. Right: Averages of all cells tested. Data are shown as the mean ± SEM. (**D**) Pairing with depolarization failed to induce LTP. Left: Sample traces during pairing. Right: Averages of all cells tested. Data are shown as the mean ± SEM. (**E**) Repatched interneurons recorded in whole-cell voltage-clamp mode show rectifying AMPARs and a negligible NMDAR-mediated component (GABA receptors blocked). Traces: Averaged EPSCs at +60 and −60 mV, showing the times at which the two components were measured. Bottom: current-voltage (*I-V*) relation of AMPAR-mediated EPSCs in six repatched interneurons (left). *I-V* relation for the NMDAR-mediated component, normalized by the AMPA EPSC at −60 mV (right).
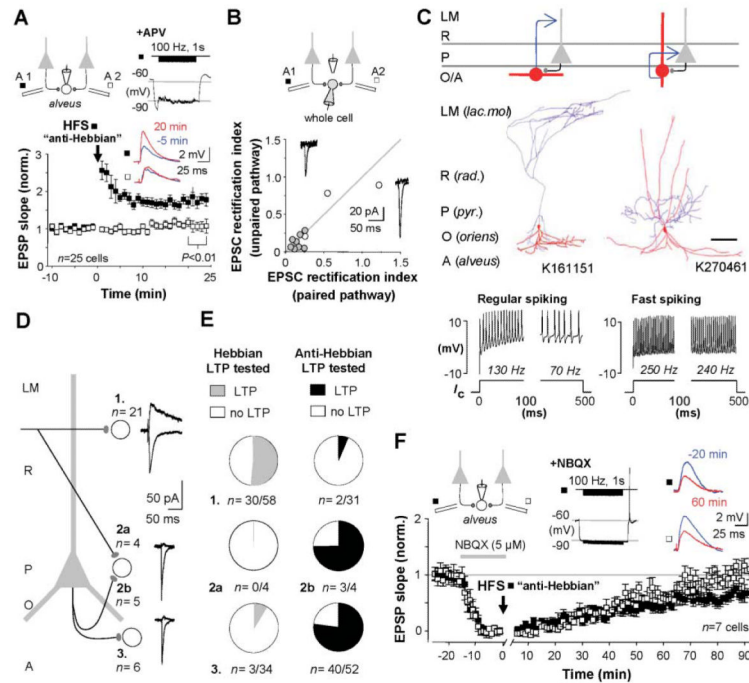
Fig. 3.
Anti-Hebbian LTP occurs in interneurons with rectifying AMPARs in the feedback circuit.
(**A**) High-frequency stimulation (HFS) paired with hyperpolarization evoked LTP in 25 out
of 31 interneurons in the oriens/alveus [NMDARs blocked with 100 μM D,L-2-amino-5-
phosphonovalerate (APV)]. Insets: Averaged EPSPs before and after LTP induction, and
membrane potential during pairing, in one interneuron. Data are shown as the mean $\pm$ SEM.
(**B**) Repatched interneurons recorded in whole-cell voltage-clamp mode revealed strongly
rectifying synaptic AMPARs (rectification index < 0.3). Gray and open symbols show cells
that did and did not exhibit LTP, respectively. Insets: Averaged EPSCs at -60 and $+60$ mV
in one cell that showed anti-Hebbian LTP. (**C**) O-LM cells were the commonest identified
interneuron type exhibiting anti-Hebbian LTP (left: schematic, with dendritic and axonal
arborizations for one cell shown in red and blue, respectively). Three fast spiking
perisomatic-projecting neurons were also identified, including a basket cell (right). Scale
bar: 200 μm. Firing patterns in response to current injection (I_c) are shown below. (**D**)
Typical layer- and pathway-specific properties of EPSCs in experiments where NMDARs
were not blocked (*n*, number of repatched interneurons). Interneurons were recorded in the
stratum radiatum (1), stratum pyramidale (2), and stratum oriens/alveus (3). (**E**) Success
rates for eliciting Hebbian or anti-Hebbian LTP at synapses made by axons illustrated in
(D). (**F**) Anti-Hebbian LTP requires activation of AMPA/kainate receptors. HFS stimulation
of one pathway (filled symbols) was paired with hyperpolarization in NBQX (5 μM) (inset).
After wash-out, EPSPs in both pathways recovered at the same rate. Inset: Averaged EPSPs
before pairing (blue) and after recovery (red) in the two pathways in one experiment. Data
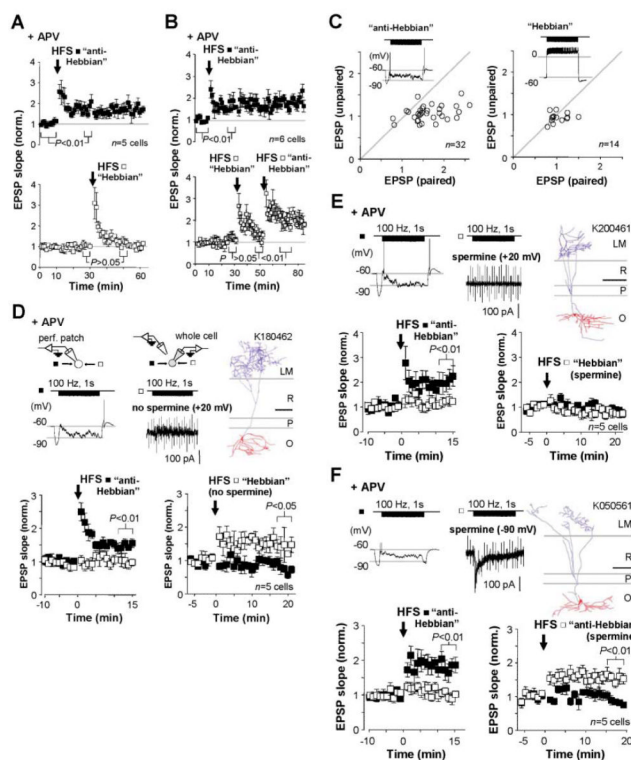are shown as the mean $\pm$ SEM.

Fig. 4.
Intracellular polyamines determine the voltage dependence of anti-Hebbian LTP. (**A**) Postsynaptic depolarization prevents LTP induction. Data from cells recorded in perforated patch mode, showing LTP induced by pairing high-frequency stimulation (HFS) of one pathway with hyperpolarization (top, "anti-Hebbian"), and failure to induce LTP by pairing the other pathway with depolarization (bottom, "Hebbian"). NMDARs were blocked throughout. Data are the mean ± SEM. (**B**) In six other cells, the second pathway was subsequently paired with hyperpolarization, yielding anti-Hebbian LTP in all cases. Data are the mean ± SEM. (**C**) Baseline-normalized EPSP slopes plotted against one another 20 min after anti-Hebbian (left) and Hebbian (right) pairing. Insets: Sample membrane potential traces during pairing. (**D**) Anti-Hebbian LTP was first induced in one pathway (left, filled symbols). The interneuron was then repatched in whole-cell mode with a polyamine-free pipette solution. HFS delivered to the second pathway (right, open symbols) paired with postsynaptic depolarization (+20 mV) induced LTP. Top: Voltage (left) and current (middle, with seal resistance test artefacts) traces during pairing, and one O-LM cell identified among five interneurons in the sample (right; scale bar: 200 μm). (**E**) Intracellular spermine blocked LTP induction in the second pathway when paired with depolarization. Top: As in (D). (**F**) LTP was induced with intracellular spermine when paired with hyperpolarization (−90 mV). Top: As in (D) and (E). Data in (D), (E), and (F) (bottom panels) are shown as the mean ± SEM.